Synthesis, Structure, and Reactivity of Chiral Rhenium *N*-Pyrrolyl Complexes $[(\eta^5\text{-}C_5H_5)Re(NO)(PPh_3)(\overline{NCR=CR'CH=CH})]$; Regiochemistry of Electrophilic Addition and Unprecedented Rearrangements to Carbon-Ligated Species

Todd J. Johnson, Luke J. Alvey, Monika Brady, Charles L. Mayne, Atta M. Arif, and J. A. Gladysz*

Abstract: Reaction of [{Re}(OTf)] (**1**; {Re} = $(\eta^5\text{-}C_5H_5)Re(NO)(PPh_3)$) and potassium pyrrolide gives the *N*-pyrrolyl complex $[\{Re\}(\overline{NCH=CHCH=CH})]$ (**2**, 88%). Reactions of **2** with $(CF_3CO)_2O$/$N(C_2H_5)_3$ and $CH_3O_2CC{\equiv}CCO_2CH_3$ give 3- and 2-substituted pyrrolyl complexes $[\{Re\}(\overline{NCR=CR'CH=CH})]$, respectively (**3**, R/R' = H/$COCF_3$, 77%; **5**, R/R' = $C(CO_2CH_3)=CHCO_2CH_3$/H, 69–87%). Free pyrrole is much less reactive towards these reagents. Reactions of **2** and TfOH or $HBF_4{\cdot}OEt_2$ give the 2*H*-pyrrole adducts $[\{Re\}(\overline{N=CHCH=CHCH_2})]^+X^-$ (**7**$^+X^-$; 89–83%). At 0–25 °C in CH_2Cl_2, these rearrange to the carbon-ligated tautomers $[\{Re\}(\overline{C=NHCH=CHCH_2})]^+X^-$ (**8**$^+X^-$) and then $[\{Re\}(\overline{C=NHCH_2CH=CH})]^+X^-$ (**9**$^+X^-$; 72–96 h, 90–96%). Reaction of **1** and pyrrole in refluxing toluene gives **8**$^+$TfO$^-$ and then **9**$^+$TfO$^-$ (92%). However, **1** and pyrrole react too slowly in CH_2Cl_2 to be intermediates in the conversion of **7**$^+$TfO$^-$ to **9**$^+$TfO$^-$. Reaction of **9**$^+$TfO$^-$ and KH gives the *C*-pyrrolyl complex $[\{Re\}(\overline{C=CHCH=HNCH})]$ (68%), which adds TfOH to give **9**$^+$TfO$^-$. Mechanistic aspects of the preceding reactions are discussed. The crystal structures of **2** and **9**$^+$TfO$^-$ are determined, and the NC_4H_x ligand conformations analyzed with extended Hückel MO calculations.

Keywords
electrophilic additions · *N*-pyrrolyl complexes · rearrangements · rhenium compounds

Introduction

A variety of transition metal *N*-pyrrolyl complexes, $[L_nM(\overline{NCH=CHCH=CH})]$, have been synthesized.[1] However, to our knowledge the reactivity of the *N*-pyrrolyl ligand has remained unexplored. This "tabula rasa" is surprising from several standpoints. For example, pyrrole rings or derivatives thereof occur in many organic natural products.[2] *N*-pyrrolyl complexes would seem to offer rich opportunities in synthesis, such as enhanced reactivity toward electrophiles,[2a] altered regiochemistry of electrophile attack,[3] and—in nonracemic adducts of chiral metal fragments—enantioselective constructs.[4] Furthermore, pyrroles are building blocks for many important materials, such as the conducting polymer polypyrrole,[5] and modified porphyrins.[6] Finally, pyrrole moieties are ubiquitous in fossil fuels, and there is considerable interest in developing improved, metal-based hydrodenitrogenation (HDN)[7] technologies for their removal.

We have had an ongoing interest in the reactivity of adducts of the chiral rhenium fragment $[(\eta^5\text{-}C_5H_5)Re(NO)(PPh_3)]^+$ ($\{Re\}^+$) and unsaturated nitrogen donor ligands. In particular, we have found that neutral enamido complexes [{Re}(N(R)CH=CHR')] can undergo highly diastereoselective electrophilic (E^+) attack β to nitrogen to give cationic imine complexes $[\{Re\}(N(R)=CHCHR'E)]^+$.[8] These can in turn be elaborated to free amines of high enantiomeric purities. Thus, we set out to prepare *N*-pyrrolyl complexes of $\{Re\}^+$, with the initial objective of developing similar chemistry. As described below, such species in fact exhibit enhanced reactivity towards electrophiles. In one case, attack occurs at the 3 position, β to nitrogen—as opposed to the 2 (α) position favored with free pyrrole. Furthermore, protic electrophiles trigger remarkable rhenium–carbon bond-forming rearrangements that ultimately give dearomatized iminoacyl derivatives of $\{Re\}^+$, and thereby access to a *C*-pyrrolyl complex. A small portion of this work has been communicated.[9]

Results

1. Synthesis and Structure of an *N*-Pyrrolyl Complex: In a reaction similar to those used to access other *N*-pyrrolyl complexes,[1a,c–g] the triflate complex [{Re}(OTf)] (**1**)[10,11] and potassium pyrrolide (1.5 equiv)[12] were combined in THF at room temperature (Scheme 1). Workup gave the *N*-pyrrolyl complex **2** in 88% yield after crystallization. Complex **2** was bright red, air-stable, and melted without decomposition at 202 °C. It was

[*] J. A. Gladysz, T. J. Johnson, L. J. Alvey, M. Brady, C. L. Mayne, A. M. Arif
Department of Chemistry, University of Utah
Salt Lake City, Utah 84112 (USA)
Telefax: Int. code + (801)581-8433

0570-0833/95/0505-0294 $ 50.00+.25/0

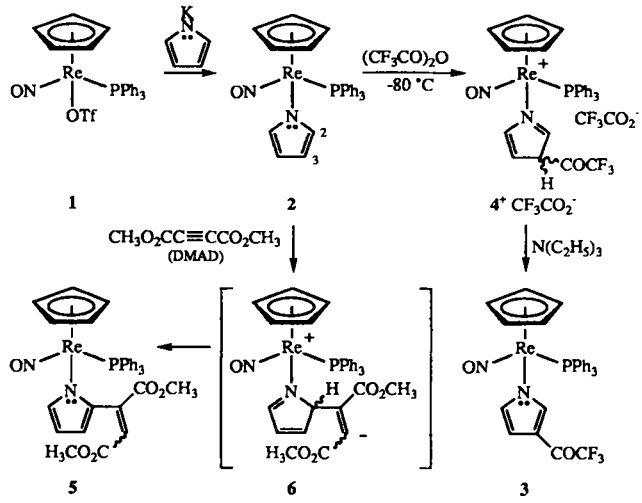

Scheme 1. Synthesis of rhenium *N*-pyrrolyl complex **2** and reactions with carbon electrophiles.

characterized, as were all new compounds isolated below, by microanalysis (see Experimental Section), and IR and NMR spectroscopy (Table 1). Similar reactions of **1** and indolide salts afforded *N*-indolyl complexes of $\{Re\}^+$, as described elsewhere.[13]

In the ^1H and ^{13}C NMR spectra of complex **2**, the NCH=CH signals had chemical shifts (δ = 6.39/5.76; 137.4/108.3) comparable to those of other *N*-pyrrolyl complexes.[1a, b, d, e, g–i] The UV/Vis spectrum exhibited a shoulder at 380 nm (ε = 930 $M^{-1}cm^{-1}$), and higherenergy absorptions characteristic of all adducts of $\{Re\}^+$. Cyclic voltammograms (0.020 M in CH_3CN, 0.10 M $(CH_3CH_2)_4N^+ClO_4^-$, 100 mVs^{-1}, ambient temperature) showed three irreversible oxidations ($E_{p,a}$ = 0.50, 1.17, 1.38 V; ferrocene reference, 0.56 V). Under identical conditions, free pyrrole was less easily, and irreversibly, oxidized ($E_{p,a}$ = 1.19 V).

As a check for any unanticipated features, the crystal structure of **2** was determined as outlined in Table 2. Refinement, described in the experimental section, gave the structures shown in Figure 1. Selected bond lengths, bond angles, and torsion angles are summarized in Table 3. Most bond lengths and angles were very similar to those found earlier for a 3-ethylindolyl complex of $\{Re\}^+$.[13] However, the conformation about the rhenium–nitrogen bond differed, as further analyzed below.

2. Reactions with Carbon Electrophiles: Pyrrole is more reactive towards electrophiles than benzene,[2a] and substitution usually occurs at C2.[3] We anticipated that **2** would be even more reactive due to the electropositive rhenium substituent at nitrogen. We also thought that the bulk of the rhenium moiety might direct attack to the more remote C3 site. Thus, **2** and trifluoroacetic anhydride were combined in CH_2Cl_2 at −80 °C (Scheme 1). Workup with triethylamine gave the 3-trifluoroacetylpyrrolyl complex **3** in 77% yield. The position of substitution was established as described below.

This transformation would be expected to involve the intermediate $\mathbf{4}^+CF_3CO_2^-$ (Scheme 1), which can be viewed as a complex of a 3*H*-pyrrole—a normally unstable type of valence tautomer.[2b] Complex $\mathbf{4}^+CF_3CO_2^-$ contains a new carbon stereocenter, and might form as a mixture of configurational diastereomers. The reaction was repeated in CD_2Cl_2 in an NMR tube. By the time the first ^{31}P NMR spectrum could be recorded (5 min, −80 °C), the resonance of **2** (δ = 17.9) had

Table 1. Spectroscopic characterization of new rhenium pyrrolyl and related complexes.

Complex	^1H NMR (δ) [a]	$^{13}C\{^1H\}$ NMR (ppm) [b]	$^{31}P\{^1H\}$ NMR (ppm) [c] IR (cm^{-1}, KBr)
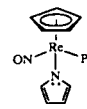 **2**	7.45-7.28 (m, 3Ph), 6.39 (t, *J*=1.8, NCH), 5.76 (t, *J*=1.8, NCHCH), 5.23 (s, C_5H_5).	PPh_3 at 135.5 (d, *J*=53.0, *i*), 134.1 (d, *J*=10.7, *o*), 130.8 (d, *J*=2.3, *p*), 128.8 (d, *J*=10.4, *m*); NC_4H_4 at 137.4 (d, *J*=1.7, NCH), 108.3 (s, NCHCH); 92.0 (d, *J*=1.4, C_5H_5).	16.8 (s) υ_{NO} 1671 vs
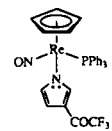 **3**	7.46-7.22 (m, 3Ph), 7.09 (dt, *J*=3.0, 1.5, 1.5, NCHCC), 6.53 (dd, *J*=2.7, 1.5, NCHCH), 6.45 (ddd, *J*=2.7, 1.5, 0.6, NCHCH), 5.25 (s, C_5H_5). [d]	PPh_3 at 133.6 (d, *J*=54.0, *i*), 133.4 (d, *J*=10.8, *o*), 130.8 (d, *J*=2.3, *p*), 128.8 (d, *J*=10.4, *m*); 172.7 (q, J_{CF}=33.2, C=O), 117.6 (q, J_{CF}=291.7, CF_3), NC_4H_3 at 146.9, 139.5 (2 s, NCH), 119.6 (s, NCHCC), 111.5 (s, NCHCH); 91.4 (s, C_5H_5). [d]	16.2 (s) [d] υ_{NO}, υ_{CO} 1669 vs, 1655 vs
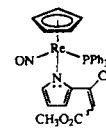 **5** [e]	7.50-7.30 (m, 3Ph), 6.38 (m, NCH), 6.37 (s, CHCO$_2$CH$_3$), 6.27 (dd, *J*=3.6, 1.5, NC(C)CH), 5.70 (dd, *J*=3.6, 2.4, NCHCH), 5.10 (s, C_5H_5), 3.88, 3.72 (2 s, CH_3).	PPh_3 at 134.7 (d, *J*=52.6, *i*), 134.2 (d, *J*=10.5, *o*), 131.1 (d, *J*=2.0, *p*), 129.1 (d, *J*=10.4, *m*); 170.1, 167.2 (2 s, C=O), 145.8 (s, NC(C)CH), 110.6 (s, CHCO$_2$CH$_3$); NC_4H_3 at 147.4 (s, NCHCH), 142.8 (s, NC(C)CH), 116.3 (s, NC(C)CH), 111.4 (s, NCHCH); 92.5 (s, C_5H_5), 52.5, 51.6 (2 s, CH_3).	16.6 (s) υ_{CO} 1708 vs υ_{NO} 1657 vs υ_{CC} 1597 vs
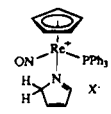 **7**$^+$ TfO$^-$/BF_4^-	8.11/8.07 (br s, N=CH), 7.44/7.42 (m, 9H of 3Ph), 7.28/7.33 (br d, *J*=5.6, *3.4*, *3.4*, CHHʹCHʹ), 7.16/7.18 (br t, *J*=7.8, 6H of 3Ph), 6.42/6.41 (br d, *J*=5.6, *1.2*, *1.2*, *1.0*, N=CHCH), 5.56/5.55 (s, C_5H_5), 4.43/4.42 (br d, *J*=26.6, *3.4*, *1.2*, CHH), 4.50/4.49 (br d, *J*=26.6, *3.4*, *1.2*, CHHʹ). [f]	PPh_3 at 132.9/133.6 (d, *J*=10.6/10.8, *o*), 131.1/131.8 (d, *J*=2.6/2.6, *p*), 130.6/131.9 (d, *J*=55.8/55.4, *i*), 128.9/129.6 (d, *J*=10.6/10.6, *m*); NC_4H_4 at 177.9/178.6 (d, *J*=1.8/1.8, C=N), 154.4/154.9 (s, CCH$_2$), 129.5/130.2 (s, N=CC), 77.7/78.4 (s, CH_2); 92.1/92.7 (s, C_5H_5). [f]	16.3/16.3 (s) υ_{NO} 1690/1681 vs (TfO$^-$/BF_4^-)
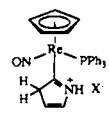 **8**$^+$ TfO$^-$/BF_4^-	11.55/10.73 (br s, NH), 7.51/7.51 (m, 9H of 3Ph), 7.30/7.28 (m, 6H of 3Ph), 6.76/6.75 (dd, *J*=3.9, 1.8, *1.8*, *1.5*, NHCH), 5.92/5.93 (dd, *J*=3.9, 2.4, *2.4*, *1.2*, CHHʹCH), 5.63/5.61 (s, C_5H_5), 3.87/3.88 (dd, *J*=26.1, 2.4, *1.8*, *1.8*, CHH), 3.02/3.06 (dd, *J*=26.1, 2.4, *1.8*, *1.8*, CHHʹ).	PPh_3 at 133.3/133.3 (d, *J*=10.6/10.8, *m*), 132.6/132.5 (d, *J*=57.0/57.5, *i*), 131.8/131.8 (d, *J*=2.6/2.6, *p*), 129.5/129.6 (d, *J*=10.9/10.9, *o*); NC_4H_4 at 227.9/228.4 (d, *J*=7.8/8.1, C=N), 133.9/134.0, 123.7/123.7 (2 s, CH), 58.2/58.1 (s, CH_2); 94.2/94.3 (s, C_5H_5).	13.8/13.7 (s) (TfO$^-$/BF_4^-)
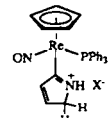 **9**$^+$ TfO$^-$/BF_4^-	10.25/9.45 (br s, NH), 7.50/7.51 (m, 9H of 3Ph), 7.22/7.29 (m, *J*=7.8, 6H of 3Ph), 6.71/6.72 (dq, *J*=5.4, 1.5, *1.5*, *1.5*, CHHʹCH), 6.65/6.69 (dq, *J*=5.4, 1.5, *1.2*, *1.2*, ReCCH), 5.61/5.59 (s, C_5H_5), 4.58/4.57 (dm, *J*=24.9, 1.5, *1.5*, *1.2*, CHH), 4.44/4.45 (dm, *J*=24.9, 1.5, *1.5*, *1.2*, CHHʹ).	PPh_3 at 133.3/133.3 (d, *J*=10.6/10.8, *m*), 133.1/132.8 (d, *J*=57.1/57.0, *i*), 131.6/131.7 (d, *J*=2.6/2.5, *p*), 129.3/129.4 (d, *J*=10.9/11.2, *o*); NC_4H_4 at 220.6/221.4 (d, *J*=7.8/8.0, C=N), 141.9/141.8, 139.9/140.2 (2 s, CH), 63.3/63.4 (s, CH_2); 94.0/94.0 (s, C_5H_5).	14.5/14.6 (s) υ_{NO} 1687/1685 vs $\upsilon_{C=N}$ 1560/1560 m (TfO$^-$/BF_4^-)
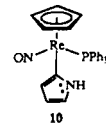 **10**	7.64 (br s, NH), 7.40-7.20 (m, 3Ph), 6.64 (dd, *J*=2.7, *2.4*, *1.2*, NHCH), 5.89 (q, *J*=2.7, *2.7*, *2.0*, NHCHCH), 5.37 (m, *J*=2.7, *2.4*, *1.2*, ReCCH), 5.18 (s, C_5H_5).	PPh_3 at 136.7 (d, *J*=52.7, *i*), 134.1 (d, *J*=10.6, *o*), 130.5 (d, *J*=2.2, *p*), 128.6 (d, *J*=10.3, *m*); NC_4H_4 at 285.7 (d, *J*=7.1, ReC), 121.4, 119.7 (2 s, ReCCCC), 108.7 (s, ReCCC); [g] 91.1 (s, C_5H_5).	19.4 (s) υ_{NO} 1638 vs

[a] 300 MHz, CD_2Cl_2, ambient temp., and internal $Si(CH_3)_4$ ref. unless noted. *J* in Hz, multiplicities correspond to peak *appearance*. Italicized couplings determined or verified from homonuclear decoupling experiments. [b] 75 MHz, CD_2Cl_2, ambient temp., and internal $Si(CH_3)_4$ ref. unless noted; $J(^{13}C,^{31}P)$/Hz unless noted. Gated decoupled $^{13}C\{^1H\}$ NMR spectra of **2**, $\mathbf{7}^+X^-$, $\mathbf{8}^+X^-$, and $\mathbf{9}^+X^-$ showed multiplicities consistent with the assignments given. Resonances of PPh carbons assigned as described in ref. [45]. The CF_3 resonance of $\mathbf{7}^+TfO^-$ was observed (120.1, q, J_{CF} = 320), but those of $\mathbf{8}^+TfO^-$ and $\mathbf{9}^+TfO^-$ were not. [c] 121 MHz, CD_2Cl_2, ambient temp., and external 85% H_3PO_4 ref. [d] $CDCl_3$, ^1H NMR at 70 °C. [e] Data provisionally assigned to the *Z* C=C isomer; see ref. [14b]. [f] −70 °C. ^1H resonances at δ = 4.43–4.42 and 4.50–4.49 appear under some conditions as a pseudodoublet at 4.47. [g] Assigned on the basis of trends in 2-lithiopyrroles; see ref. [2], p. 41.

Table 2. Summary of crystallographic data for **2** and **9**$^+$TfO$^-$.

	2	**9**$^+$TfO$^-$
molecular formula	$C_{24}H_{24}N_2OPRe$	$C_{28}H_{25}F_3N_2O_4PReS$
molecular weight	609.679	759.756
crystal system	monoclinic	monoclinic
space group	$P2_1/n$ (No. 14)	$P2_1/n$ (No. 14)
cell dimensions (18, 16 °C)		
a, Å	10.866(2)	11.311(1)
b, Å	16.029(3)	18.038(1)
c, Å	13.559(2)	13.946(1)
β, deg	91.52(2)	97.04(1)
V, Å^3	2360.72	2823.89
Z	4	4
d_{calcd}, g cm^{-3}	1.715 (18 °C)	1.787 (16 °C)
d_{obs}, g cm^{-3} (CCl_4/CH_2I_2)	1.72 (22 °C)	1.76 (22 °C)
crystal dimensions, mm	0.27 × 0.24 × 0.16	0.26 × 0.25 × 0.21
diffractometer	Syntex PĪ	Syntex PĪ
radiation, Å	$\lambda(Mo_{K\alpha})$, 0.71073	$\lambda(Mo_{K\alpha})$, 0.71073
data collection method	θ–2θ	θ–2θ
scan speed, deg/min	3.0	3.0
reflections measured	4534	5536
range/indices ($h\,k\,l$)	0, 12; 0, 19; −16, 16	0, 13; 0, 21; −16, 16
2θ limit, deg	4.0–50.0	3.0–50.0
standard reflections check	1 X-ray hour	98
total unique data	4297	5156
observed data, $I > 3\sigma(I)$	3177	3934
abs. coefficient, cm^{-1}	53.043	45.427
min. transmission, %	56.27	86.20
max. transmission, %	99.98	99.99
no. of variables	385	361
goodness of fit	0.956	2.58
$R = \Sigma\|\|F_o\| - \|F_c\|\|/\Sigma\|F_o\|$	0.0261	0.0206
$R_w = \Sigma\|\|F_o\| - \|F_c\|\|w^{1/2}/\Sigma\|F_o\|w^{1/2}$	0.0359	0.0241
Δ/σ (max)	0.024	0.002
$\Delta\rho$ (max), e Å^{-3}	1.253	0.359

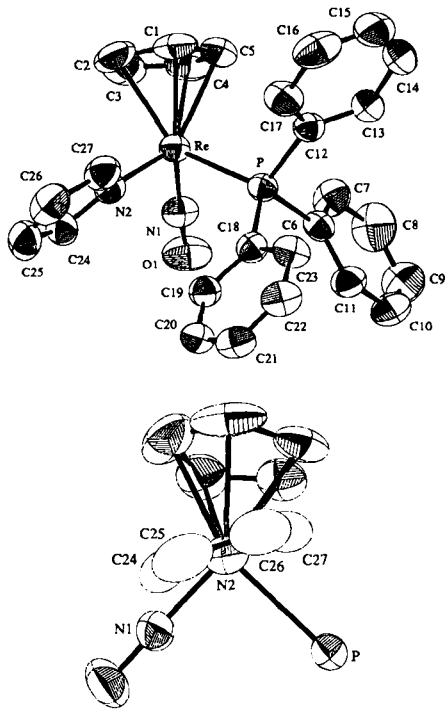

Fig. 1. Structure of the *N*-pyrrolyl complex **2**: top: numbering diagram; bottom: Newman-type projection down the N2–Re bond with phenyl rings omitted.

Table 3. Selected bond lengths (Å), bond angles (°), and torsion [a] angles (°) in **2** and **9**$^+$TfO$^-$ [b].

	2	**9**$^+$TfO$^-$		**2**	**9**$^+$TfO$^-$
Re–P	2.361(1)	2.3854(7)	Re-N2-C27	126.9(5)	
Re–N1	1.756(5)	1.763(3)	C1-C2-C3	107.1(8)	107.7(3)
Re–N2	2.094(5)		C2-C3-C4	109.3(8)	108.5(3)
Re–C24		2.046(3)	C3-C4-C5	107.1(9)	108.0(3)
N1–O1	1.203(6)	1.182(3)	C1-C5-C4	110.2(8)	108.2(3)
N2–C24	1.362(8)	1.314(4)	C2-C1-C5	106.3(8)	107.5(3)
N2–C27	1.358(9)	1.453(4)	C24-N2-C27	106.3(6)	114.0(3)
Re–C1	2.299(6)	2.274(3)	N2-C24-C25	110.3(8)	105.1(3)
Re–C2	2.324(8)	2.297(3)	C24-C25-C26	106.6(7)	109.5(3)
Re–C3	2.304(8)	2.303(3)	C25-C26-C27	107.3(7)	110.2(3)
Re–C4	2.262(7)	2.333(3)	N2-C27-C26	109.5(8)	101.2(3)
Re–C5	2.238(7)	2.299(3)	N2-C27-H24		116.5
C24–C25	1.37(1)	1.476(4)	N2-C27-H23		121.3
C25–C26	1.37(1)	1.323(5)	C26-C27-H24		106.3
C26–C27	1.38(1)	1.469(6)	C26-C27-H23		101.7
O2–H25		2.31	H23-C27-H24		107.3
O3–H25		2.77	O3-H25-N2		107.8
P-Re-N1	89.7(2)	92.4(1)	P-Re-N2-C24	122.8(5)	
P-Re-N2	92.8(1)		P-Re-C24-C25		103.3(4)
P-Re-C24		92.5(1)	P-Re-N2-C27	295.3(5) [c]	
Re-N1-O1	176.3(5)	175.8(2)	P-Re-C24-N2		275.2(4) [d]
Re-N2-C24	126.5(5)		N1-Re-N2-C24	32.7(5)	
Re-C24-N2		129.3(2)	N1-Re-C24-C25		10.7(4)
N1-Re-N2	98.0(2)		N1-Re-N2-C27	205.2(5) [e]	
N1-Re-C24		93.6(1)	N1-Re-C24-N2		182.6(4) [f]

[a] See ref. [27c]. [b] Since hydrogen atom positions were not refined in **9**$^+$TfO$^-$, estimated standard deviations are not given for the corresponding metrical parameters. [c] Or −64.7(5). [d] Or −84.8(4). [e] Or −154.8(5). [f] Or −177.4(4).

been replaced by three new signals (δ = 16.9, 16.8, 16.6; 18:61:21).[14a] A downfield ^{1}H resonance (δ = 7.93, brs) was also present. When the probe was warmed to room temperature, two signals remained (δ = 16.2, 15.9; 86:14). After triethylamine was added (room temperature), only the δ = 16.2 resonance remained. A ^{1}H NMR spectrum showed that complete conversion to **3** had occurred. No reaction was observed when free pyrrole and trifluoroacetic anhydride were similarly combined in CD_2Cl_2 at −100 °C. When the probe was warmed to −80 °C, 35% of the pyrrole was consumed after 50 min. Hence, **2** is more reactive than pyrrole towards trifluoroacetic anhydride.

Next, **2** and DMAD[10] were reacted in CH_2Cl_2 at room temperature (Scheme 1). Workup gave the 2-substituted pyrrolyl complex **5** in 69–87% yields as 94–90:6–10 mixtures of C=C geometric isomers.[14b] The carbon connectivity was established by a 2D INADEQUATE NMR pulse sequence,[15, 16] which confirmed the assignments in Table 1. Other *N*-substituted pyrroles and DMAD react similarly.[17] Complex **2** and DMAD were also combined in an NMR tube in CD_2Cl_2 at low temperature. After 1.5 h at −30 °C, 38% conversion to **5** had occurred (72:28 C=C isomer mixture).

The formation of **5** would be expected to involve the zwitterionic intermediate **6** (Scheme 1), and a subsequent proton shift. The less electrophilic alkenes acrolein, acrylonitrile, and diethyl maleate gave no reaction after 2 days under comparable conditions. Also, free pyrrole and DMAD were combined in CD_2Cl_2 in an NMR tube, in concentrations analogous to those in the above reaction with **2**. No reaction was observed at 40 °C. Hence, **2** is much more reactive than pyrrole towards DMAD.

In the ^{13}C NMR spectra of **2** and **5** the C2 signals (δ = 137.4–147.4) were distinctly downfield of the C3 signals (δ = 108.3–116.3). Other *N*-pyrrolyl complexes show similar trends (δ = 129–137 and 104–109).[1b, c, h, i] Complex **3** exhibited two downfield (δ = 146.9/139.5) and two upfield (δ = 119.6/117.6) pyrrolyl ligand resonances. Accordingly, these were assigned to C2/C2′ and C3/C3′. A DEPT pulse sequence[18] established that the trifluoroacetyl group was attached to an upfield carbon (δ = 119.6), and thus indicated the presence of a 3-substituted pyrrolyl ligand.

0570-0833/95/0505-0296 $ 50.00+.25/0

3. Reactions and Rearrangements Involving Protic Electrophiles: The strong acids TfOH and $HBF_4 \cdot OEt_2$ were added to separate ether solutions of **2** (Scheme 2). The cationic adducts $\mathbf{7}^+X^-$ ($X^- = TfO^-$, BF_4^-) precipitated as analytically pure yellow powders in 89–83% yields. These compounds, formed by protonation at C2, can be viewed as complexes of the unisolable pyrrole tautomer 2*H*-pyrrole.[2b]

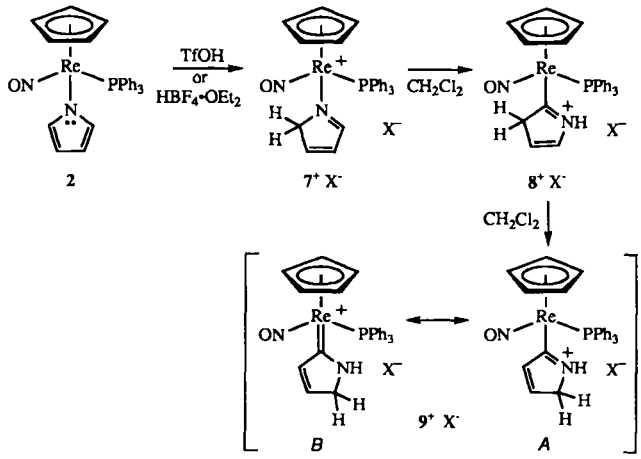

Scheme 2. Reactions of *N*-pyrrolyl complex **2** with protic electrophiles.

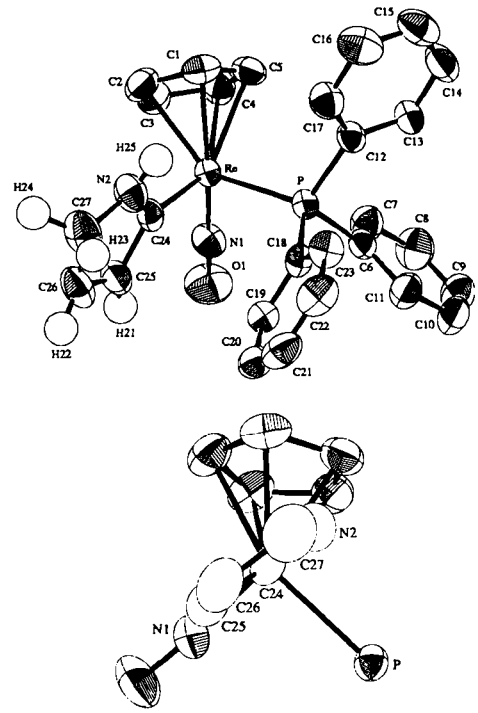

Fig. 2. Structure of the cation of $\mathbf{9}^+TfO^-$: top: numbering diagram; bottom: Newman-type projection down the C24–Re bond with phenyl rings omitted.

The structures of $\mathbf{7}^+X^-$ were established as follows: First, the $\tilde{\nu}_{NO}$ values in the IR spectra (1690–1681 cm^{-1}) and the downfield N=CH chemical shifts in the ^1H and ^{13}C NMR spectra ($\delta = 8.11-8.07$ (brs); $\delta = 177.9-178.6$ (d, $^3J_{CP} = 1.8$ Hz)) were similar to those of cyclic and acyclic imine complexes of $\{Re\}^+$.[19] Second, the CH_2 ^{13}C resonances ($\delta = 77.7-78.4$) were typical of 2*H*-pyrrole derivatives, and downfield of those of 3*H*-pyrroles.[2b] Also, the CH ^{13}C resonances were within 6 ppm of those of the 2*H*-pyrrole salt $[HN{=}CHCH{=}CHCH_2]^+HSO_4^-$.[20] Finally, a 2D INADEQUATE NMR pulse sequence showed that the CH_2 group was connected to only one other carbon.[15, 16]

Unexpectedly, $\mathbf{7}^+X^-$ sequentially rearranged to two new species ($\mathbf{8}^+X^-$, $\mathbf{9}^+X^-$) in CH_2Cl_2 or CD_2Cl_2 . NMR spectra showed that $\mathbf{7}^+TfO^-$ isomerized more rapidly than $\mathbf{7}^+BF_4^-$, but both processes were slow at −40 °C. The yields of $\mathbf{8}^+TfO^-$ and $\mathbf{8}^+BF_4^-$ maximized at 82–84% and 25–34% (4–6 h, room temperature), respectively; additional rate data are given below. After 4 days, workups of preparative reactions gave $\mathbf{9}^+X^-$ as red powders in 90–96% yields. These were assigned as the *C*-ligated *N*-protonated iminoacyl complexes $\mathbf{9}^+X^-$ (Scheme 2) on the basis of the $\nu_{C=N}$ band (1560 cm^{-1}) in the IR spectrum, downfield ReC=N ^{13}C NMR signals ($\delta = 220.6-221.4$ (d, $^2J_{CP} = 7.8-8.0$ Hz)), and several types of NMR decoupling experiments (Table 1).

In order to verify these assignments, the crystal structure of $\mathbf{9}^+TfO^-$ was determined as outlined in Table 2. Refinement gave the partial structures in Figure 2 and the data in Table 3. The distance between one triflate oxygen (O2) and the C=NH proton (H25), 2.31 Å, was within the range associated with N···H···O hydrogen bonds.[21] The corresponding O2–N2 distance was 3.24 Å.

Complex $\mathbf{8}^+X^-$ gave NMR data similar to that of $\mathbf{9}^+X^-$ (Table 1). In accord with analogous decoupling experiments, it was assigned as the tautomer shown in Scheme 2.[22] Thus, the 2*H*-pyrrole complexes $\mathbf{7}^+X^-$ undergo spontaneous and to our knowledge unprecedented rearrangements in which rhenium–nitrogen bonds are replaced by rhenium–carbon bonds. We therefore sought data that would help define the mechanisms of these processes.

4. Synthesis of a *C*-Pyrrolyl Complex: We noted that the deprotonation of $\mathbf{9}^+X^-$ might give a potential intermediate in the preceding rearrangements, the *C*-pyrrolyl complex **10** (Scheme 3). Thus, $\mathbf{9}^+TfO^-$ and KH were combined in THF at room temperature. Workup gave **10** in 68% yield as a slightly air-sensitive red powder. Complex **10** exhibited a lower $\tilde{\nu}_{NO}$ value than the *N*-pyrrolyl isomer **2** (1638 vs. 1671 cm^{-1}), and a downfield ReC ^{13}C NMR signal ($\delta = 285.7$ (d, $^2J_{CP} = 7.1$ Hz)). To our knowledge, only a few *C*-pyrrolyl complexes have been characterized. These include adducts of the ruthenium and osmium fragments $M(CO)_2(PPh_3)_2(Cl)$,[23] and the rhodium fragment $(\eta^5\text{-}C_5Me_5)Rh(PMe_3)(H)$.[1j]

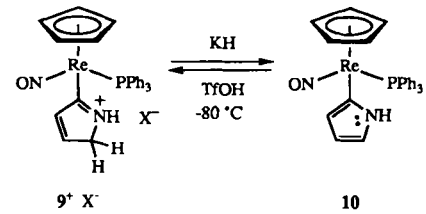

Scheme 3. Synthesis of a *C*-pyrrolyl complex.

Complex **10** and TfOH were combined in CD_2Cl_2 at −80 °C. The precursor to **10**, $\mathbf{9}^+TfO^-$, was regenerated in quantitative yield in less than 5 min, as assayed by ^1H and ^{31}P NMR. Hence, **10** cannot be a precursor to the less stable tautomer $\mathbf{8}^+TfO^-$, which only slowly isomerizes to $\mathbf{9}^+TfO^-$ at −40 °C. However, **10** remains a viable intermediate in the conversion of $\mathbf{8}^+TfO^-$ to $\mathbf{9}^+TfO^-$. This process could also occur without proton dissoci-

ation by a [1,3] sigmatropic shift or two [1,5] sigmatropic shifts, as shown for related compounds below.

5. Reactions Involving Free Pyrrole: We sought to probe the possibility that 7^+TfO^- might be a source of triflate complex **1** and free 2*H*-pyrrole or 1*H*-pyrrole. As shown in Scheme 4, subsequent electrophilic attack of **1** at C2 of 1*H*-pyrrole would give

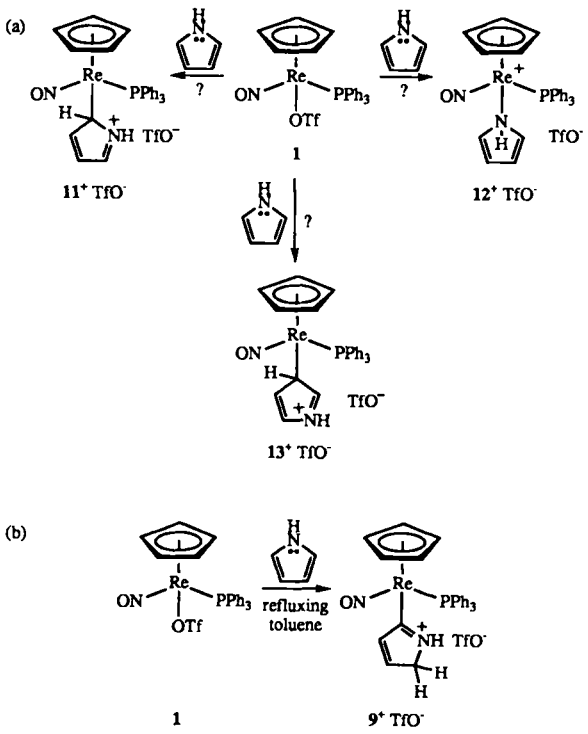

Scheme 4. Reaction of triflate complex **1** and free pyrrole: a) possible initial steps; and b) observed product (8^+TfO^- and traces of 7^+TfO^- detected at partial conversion).

the carbon-bonded complex 11^+TfO^-, which could convert by proton shifts to 8^+TfO^- and 9^+TfO^-. Alternatively, reaction could occur at the pyrrole nitrogen to give the 1*H*-pyrrole complex 12^+TfO^-. A third possibility, attack at C3 to give 13^+TfO^-, is also depicted. Interestingly, pyrrole undergoes H/D exchange at nitrogen much more rapidly than at C2 or C3.[2c] Thus, the least basic site is the more reactive towards certain electrophiles.

In fact, the direct reaction of **1** and excess pyrrole in refluxing toluene gave 9^+TfO^- in 92% yield after workup (Scheme 4b). To our knowledge, this represents the first example of a transition metal electrophile attacking a pyrrole to give a product with a metal–carbon σ bond. Related reactions with mercury electrophiles have been reported.[24] In a separate experiment, aliquots were assayed by ^1H NMR in CD_2Cl_2. This established the intermediacy of 8^+TfO^- and—unexpectedly—the formation of some 7^+TfO^-. Thus, after 1 min at 100 °C, a 68:3:12:17 $1/7^+TfO^-/8^+TfO^-/9^+TfO^-$ mixture was present. After 5 and 15 min, 35:3:15:47 and 1:1:1:97 mixtures had formed. After 45 min, only 9^+TfO^- remained.

Complex **1** and pyrrole were then combined in CD_2Cl_2 (0.083 and 0.11 M) at room temperature. The reaction was monitored by ^1H and ^{31}P NMR, and the rate compared to those of the disappearance of 7^+TfO^- and $7^+BF_4^-$ under identical conditions. Data are summarized in Table 4. After 12 h, only 26% of **1** was consumed ($1/7^+TfO^-/8^+TfO^-/9^+TfO^-$/other species 74:3:9:1:13), but 7^+X^- was 92–68% isomerized. Hence, **1** and pyrrole react *too slowly* to be intermediates in the conversion of 7^+X^- to 9^+X^-. Furthermore, the generation of some *N*-ligated product, 7^+TfO^-, suggests the intermediacy—at least in part—of the 1*H*-pyrrole complex 12^+TfO^-, as further analyzed below.

6. MO Calculations: We sought to analyze aspects of the frontier molecular orbitals and solid state conformations of **2** and 9^+TfO^-. For example, the NC_4H_x moieties are approximately isosteric, with one methine group in **2** (C26) corresponding to a methylene group (C27) in 9^+TfO^-. Both ligating atoms are flanked by CH or NH groups and have comparable distances to rhenium (2.094(5) vs. 2.046(3) Å). However, as shown in Figures 1 and 2 (bottom), the NC_4H_x ligands exhibit slightly different conformations. That in **2** is rotated 20–23° in a clockwise direction, as calculated from the torsion angles in Table 3.

Although such differences could be due to packing forces, we thought there might be an electronic rationale. In particular, the rhenium fragment $\{Re\}^+$ is a strong π donor, with the d orbital HOMO shown in Figure 3 (**I**). Unsaturated ligands often adopt conformations that allow a high degree of overlap of their acceptor orbitals with this HOMO. Thus, extended Hückel MO calculations were conducted on model compounds with PH_3 instead of PPh_3 ligands (**2**-PH_3, 9^+-PH_3; see Experimental Section). This protocol reliably locates conformational minima in related compounds.[25–27] Figure 4 shows the variation in energy as the NC_4H_x ligands were rotated through 360°. Data points were calculated every 2° near the minima.

Table 4. Product distributions from NMR monitored reactions (0.083 M in 7^+X^- or **1**, CD_2Cl_2, 25 °C) [a].

	Isomerization of 7^+TfO^-			Isomerization of $7^+BF_4^-$			Reaction of **1** and pyrrole [b]				
Time (h)	7^+TfO^-	8^+TfO^-	9^+TfO^-	$7^+BF_4^-$	$8^+BF_4^-$	$9^+BF_4^-$	**1**	7^+TfO^-	8^+TfO^-	9^+TfO^-	Other
0	100	0	0	100	0	0	100	0	0	0	0
2	30	66	4	65	22	13	88	2	2	0	8
4	13	82	5	53	25	22	86	2	4	0	8
6	11	74	15	51	19	30	84	3	5	0	8
9	10	69	21	35	19	46	80	2	8	1	9
12	8	61	31	32	19	49	74	3	9	1	13
28	1	40	59	1	14	85	67	2	15	2	14
50	0	30	70	0	2	98	47	3	18	7	25
75	0	0	100	0	0	100	32	3	20	14	31

[a] A reviewer has noted that the fractional decreases in reactant and intermediate concentrations do not always appear to follow simple rate laws. Several versions of these experiments have been conducted, always with qualitatively similar phenomena and rates. [b] The pyrrole concentration is 0.11 M. Cyclopentadienyl ^1H NMR chemical shifts: $7^+TfO^-/8^+TfO^-/9^+TfO^-$ at δ = 5.55/5.64/5.61; other species at δ = 5.48, 5.36, 5.25 (major), 5.01. These chemical shifts are invariant at all time intervals and the relative ratios of the other products do not vary significantly.

0570-0833/95/0505-0298 $ 50.00+.25/0 Chem. Eur. J. 1995, 1, No. 5

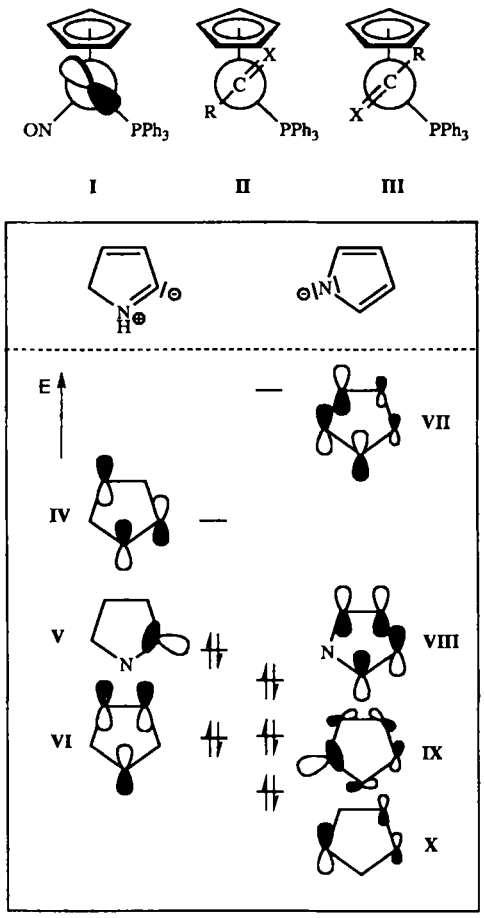

Fig. 3. Limiting conformations of -C(R)=X adducts of **I**, and frontier orbitals of NC_4H_x ligands.

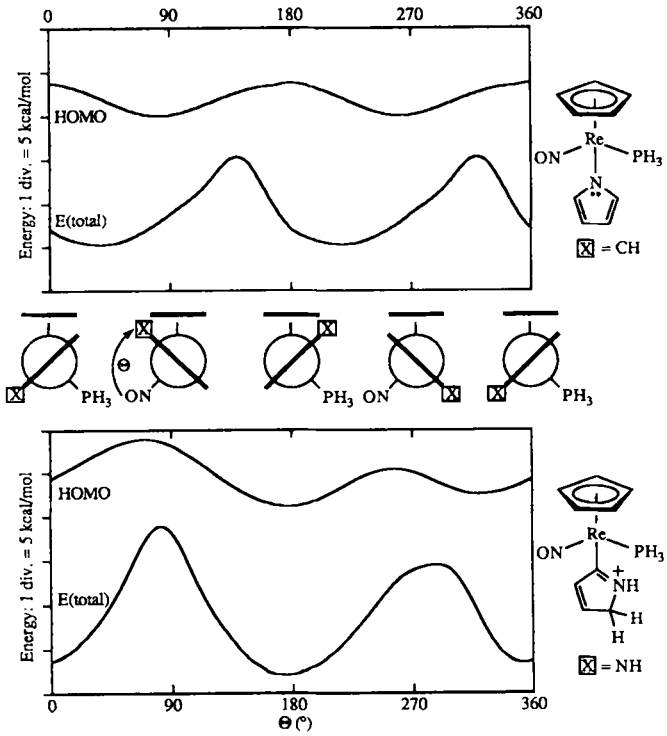

Fig. 4. Variation in total energies and HOMO energies as the NC_4H_x ligands are rotated in analogues of **2** and 9^+X^- with PH_3 ligands; calculated by the extended Hückel method as described in the Experimental Section.

Both model compounds gave two energy minima differing by approximately 180° rotations. For **2**-PH_3, these were degenerate, with ON-Re-N-C torsion angles (36°, 216°) close to those in crystalline **2** (32.7°, 205.2°).[27c] For 9^+-PH_3, a conformer with a 176° ON-Re-C=N torsion angle (**II**, Figure 3) was slightly lower in energy than one with a 350° torsion angle (**III**). Crystalline 9^+TfO^- exhibits a 182.6° ON-Re-C=N torsion angle. Hence, the calculations reproduce the solid state structures.

The frontier orbitals of the NC_4H_x ligands were calculated, and are depicted in Figure 3. The LUMO of the NC_4H_5 moiety in 9^+X^- (**IV**) had appreciable C=NH π^* character. It was much lower in energy than the LUMO of the $^-NC_4H_4$ moiety in **2** (**VII**). Thus, a stronger attractive interaction with the HOMO **I** would be anticipated. In both ligands, the HOMO or SHOMO was a σ donor orbital (**V**, **IX**). The third highest occupied $^-NC_4H_4$ orbital (**X**) featured a large p orbital coefficient on nitrogen. This would give a repulsive interaction with the HOMO of **I**, especially near ON-Re-N-C torsion angles of 0 or 180°.

The variation in HOMO energies of the model compounds are also given in Figure 4. For 9^+-PH_3, the minima of the total and HOMO energies closely coincided, consistent with the attractive frontier orbital interaction proposed above. Accordingly, at the minima the HOMO was essentially a bonding combination of orbitals of the types shown in **I** and **IV** (Fig. 3). For **2**-PH_3, the minima of the total and HOMO energies were out of phase by 46°. The locations of the HOMO minima and maxima were consistent with a dominating repulsive interaction between orbitals of the types shown in **I** and **X**. At the total energy minima, the three highest occupied orbitals did not show any electron density on the $^-NC_4H_4$ ligand. Thus, the regiochemistry of electrophilic attack upon **2** cannot be analyzed in the context of frontier orbital control.

Discussion

1. Electrophilic Attack upon Pyrrolyl Ligands: The above data show that *N*-pyrrolyl and *C*-pyrrolyl complexes of the rhenium fragment $\{Re\}^+$ are readily attacked by carbon and/or protic electrophiles. In all cases examined, rates are faster than the corresponding reactions of free pyrrole. Although there have not to our knowledge been previous reports of electrophilic additions to pyrrolyl ligands, some related investigations deserve emphasis.

For example, Hidai has found that tungsten pyrrolylimido complexes undergo facile electrophilic substitution, as illustrated in Equation (i) of Scheme 5.[3b] In each case, a C3 hydrogen is replaced. This regioselectivity has been attributed to the bulk of the *cis* chelating phosphine ligands. Pyrroles with large *N*-silyl substituents behave similarly.[3a] Also, Harman has found that the osmium fragment $[Os(NH_3)_5]^{2+}$ and pyrroles combine to give η^2-π complexes.[28] The uncomplexed, enamine-like portion of the pyrrole is readily attacked by electrophiles, as exemplified in Equation (ii) of Scheme 5.

Our data show that carbon electrophiles can attack the *N*-pyrrolyl ligand of **2** at either C2 or C3. Hence, the bulk of the rhenium fragment does not appear to be sufficient to dictate the position of substitution. Unfortunately, further analysis of the regiochemistry is complicated by ambiguities regarding kinetic and thermodynamic control. For example, by analogy to protonated pyrrole,[2c] the 2*H*-pyrrole complex 7^+X^- is likely the most stable form of protonated **2**. If 3-protonated or *N*-proto-

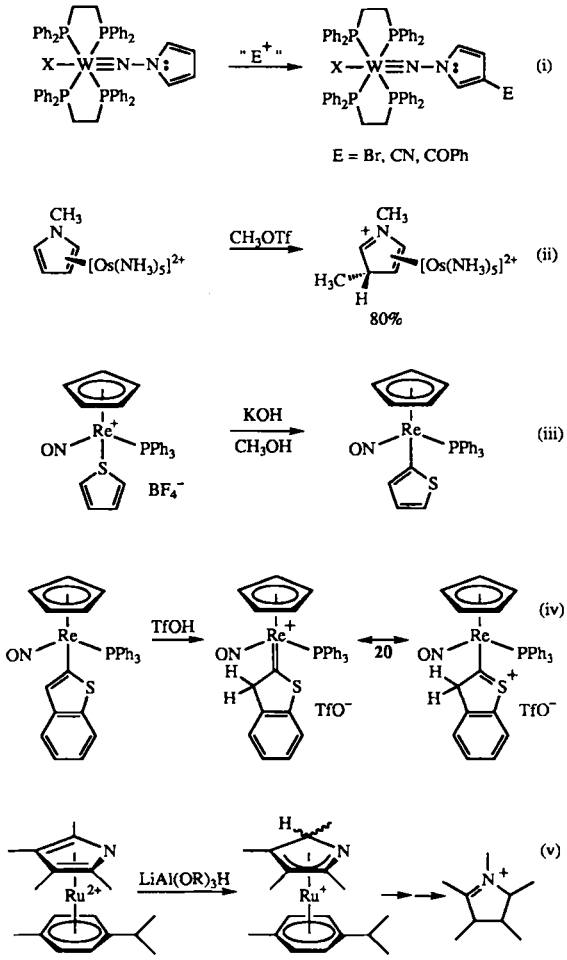

Scheme 5. Selected reactions of aromatic heterocycle complexes.

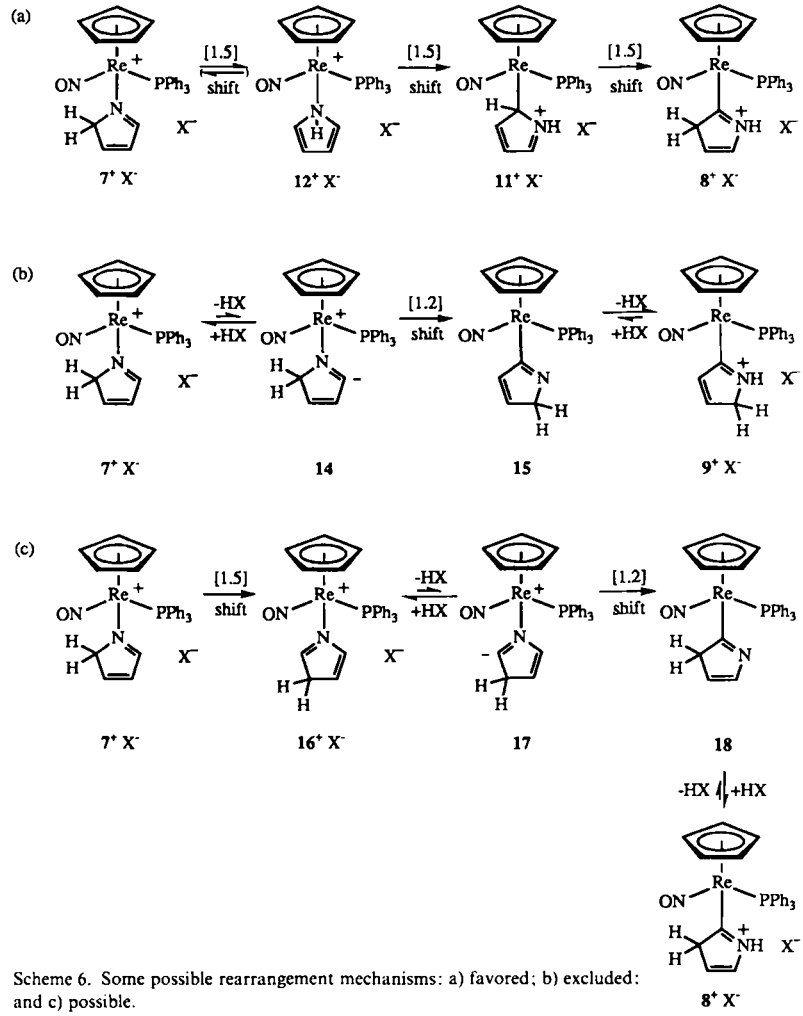

Scheme 6. Some possible rearrangement mechanisms: a) favored; b) excluded: and c) possible.

nated isomers were more stable (16^+X^-, 12^+X^-, Scheme 6), there is no obvious reason why (net) [1,5] sigmatropic shifts of CH protons of 7^+X^- to give these species would not be rapid. However, it remains possible that **2** undergoes preferential kinetic protonation at C3 or nitrogen—or even rhenium.

2. Rearrangement Mechanisms: The isomerization of nitrogen-ligated 7^+X^- to carbon-ligated 8^+X^- and 9^+X^- (Scheme 2) appears to be unprecedented. Although our data exclude several mechanisms, it is difficult to identify a compelling choice among the remaining possibilities. Of the numerous pathways considered, those in Scheme 6 are representative.[29] In mechanism (a), a formal [1,5] sigmatropic shift of a CH_2 proton gives the 1*H*-pyrrole complex 12^+X^-.[30] This less stable species could undergo a [1,5] sigmatropic shift of rhenium,[31] yielding the carbon-bonded complex 11^+X^-, or return to 7^+X^-. The reversibility of this step is suggested by the formation of some nitrogen-ligated 7^+TfO^-—which would most plausibly arise from 12^+TfO^-—in the much slower reaction of triflate complex **1** and pyrrole (Scheme 4 and Table 4). A [1,5] sigmatropic shift of the ReCH proton in 11^+X^- would then give 8^+X^-, which could isomerize to 9^+X^- as analyzed above.

As shown in Table 4, the rearrangement of 7^+X^- to 8^+X^- is more rapid when the counter anion is more basic ($TfO^- > BF_4^-$). Thus, the anion might mediate the initial CH_2 proton shift. However, the anion cannot mediate the ReCH proton shift that converts 11^+X^- to 8^+X^-. This would generate the *C*-pyrrolyl complex **10**, which, as shown in Scheme 3, reacts with acid to give 9^+X^-—the final product, as opposed to the observed kinetic product.

Another way of converting 12^+X^- to 11^+X^- would involve changing the hapticities of the cyclopentadienyl and 1*H*-pyrrole ligands from η^5 to η^1 (or η^3), and η^1 to η^5 (or η^3), respectively. In this context, several cyclopentadienyl *N*-pyrrolyl complexes have been reported, and equilibria lie in the direction of the η^1 *N*-pyrrolyl isomers.[1a,b,g] Data are not yet available for complexes with both cyclopentadienyl and 1*H*-pyrrole ligands. However, Casey has shown that closely related rhenium complexes react with PMe_3 to give adducts with η^1cyclopentadienyl ligands.[31b,c] Thus, mechanistic variants involving hapticity changes appear viable.

Coordinated ligands are often activated towards deprotonation, particularly in cationic complexes. Furthermore, there are several recent examples with heteroatomic donor ligands that involve subsequent rearrangements.[32,33] These can give metal–carbon bonds, as illustrated by Angelici's results with thiophene complexes of $\{Re\}^+$ (Eq. (iii), Scheme 5).[32] Thus, we have considered the possibility that an N=CH proton might be abstracted from 7^+X^- to give the ylide **14**, as sketched in mechanism (b) in Scheme 6.[34] Note that the abstraction of an NCH_2 proton, which is certainly much more acidic, would simply regenerate **2**.

A [1,2] sigmatropic shift of the rhenium in **14** would give the carbon-bonded iminoacyl complex **15** (Scheme 6). However, direct *N*-protonation would then generate 9^+X^-, bypassing the observed intermediate 8^+X^-. This mechanism can be salvaged

0570-0833/95/0505-0300 $ 50.00+.25/0 Chem. Eur. J. 1995, 1, No. 5

by invoking a sigmatropic shift (or shifts) of an NCH_2 proton of **15** to give the tautomer **18**. Now *N*-protonation would give the correct kinetic product, $\mathbf{8}^+X^-$. However, in our opinion this scenario seems contrived.

Alternatively, $\mathbf{7}^+X^-$ could first undergo a (net) [1,5] sigmatropic shift of a CH_2 hydrogen to give the less stable 3*H*-pyrrole complex $\mathbf{16}^+X^-$ shown in mechanism (c) (Scheme 6). A similar species, $\mathbf{4}^+CF_3CO_2^-$, must form in the reaction of **2** and trifluoroacetic anhydride (Scheme 1). Now, loss of an N=CH proton would afford the ylide **17**, which could undergo a [1,2] shift of rhenium to give **18**. Subsequent *N*-protonation would give $\mathbf{8}^+X^-$. Thus, mechanism (c) is consistent with presently available data. However, in view of the likely modest N=CH proton acidity, we presently favor mechanism (a).

3. Structural Data: The *N*-protonated iminoacyl complex $\mathbf{9}^+TfO^-$ is isoelectronic with acyl complexes of the formula [{Re}(C(R)=O)] (**19**). Two of the latter have been structurally characterized (**19a**: R = H; **19b**: R = $CH(CH_3)CH_2C_6H_5$),[25a] and show ON-Re-C=X torsion angles and rhenium–carbon bond lengths close to those of $\mathbf{9}^+TfO^-$ (176–181° vs. 182.6°;[27c] 2.055(10)–2.081(7) Å vs. 2.046(3) Å). Such bond lengths indicate appreciable double-bond character, as analyzed earlier[25a] and illustrated by resonance form *B* of $\mathbf{9}^+X^-$ in Scheme 2. The ReC=X bond in $\mathbf{9}^+TfO^-$ is longer than those in **19a,b** (1.314(4) Å vs. 1.220(12)–1.252(10) Å); this parallels trends for free imines and carbonyl compounds.[35] The crystal structure of a protonated *C*-benzothienyl adduct of $\{Re\}^+$, **20** (Eq. (iv), Scheme 5), has also been determined.[32b] It exhibits a slightly shorter rhenium–carbon bond (1.992(7) Å), but a similar ON-Re-C=X torsion angle (182.7°).[27c]

These data, and Hückel MO calculations described above and elsewhere,[25a] establish that strong attractive interactions exist between the HOMO of **I** and C=X ligand acceptor orbitals in $\mathbf{9}^+X^-$, **19a,b**, and **20**. However, as is readily visualized from Figure 3, pyrrolyl ligands are poorer π acceptors and better π donors. Thus, if the NC_4H_x moiety in **2** were to adopt a conformation analogous to that in $\mathbf{9}^+TfO^-$, attractive frontier orbital interactions would be weaker, and repulsive interactions would be stronger. Accordingly, the NC_4H_x group rotates 20–23° clockwise from that in $\mathbf{9}^+TfO^-$. This also removes an eclipsing interaction of the nitrosyl ligand and an NCH proton, directing the latter into the spacious interstice between the nitrosyl and cyclopentadienyl groups.[26] Interestingly, the analogous 3-ethylindolyl complex shows an additional 39° clockwise rotation (∢ON-Re-N-C 70.9°, 243.7°).[13, 27c] In this compound, a much larger fused benzenoid ring would otherwise sterically interact with the nitrosyl ligand.

As illustrated by **II** and **III** in Figure 3, there are *two* rhenium–carbon conformations of $\mathbf{9}^+TfO^-$, **19a,b**, and **20** that maximize overlap of the HOMO of **I** and the C=X ligand acceptor orbitals. In **III**, the ON-Re-C=X torsion angle is 0°. Since all of these compounds, and numerous related iron acyl complexes of the formula $[(\eta^5\text{-}C_5H_5)Fe(CO)(PPh_3)(C(R)=O]$, crystallize in the conformation **II**, it has been widely assumed that **III** is less stable.[36, 37] There has been a lively controversy regarding the origin of this trend.[36] The energy difference calculated for $\mathbf{9}^+\text{-}PH_3$ in Figure 4 is not large enough to interpret. However, since **II** and **III** are essentially isosteric for $\mathbf{9}^+TfO^-$, an electronic basis for the stability order is likely.

4. Prospective: The new reactions reported above provide many attractive leads for future research. For example, the facile generation of dearomatized pyrrole derivatives from **1** or **2** (Schemes 2 and 4) suggests new approaches to transition metal promoted hydrodenitrogenation processes. In particular, the resulting C=N linkages should be susceptible to hydrolysis, ring opening, and related degradative reactions. In a complementary study, Rakowski-DuBois et al. have shown that nucleophiles can attack cationic η^5-pyrrolyl complexes to give dearomatized adducts, as illustrated in Equation (v) of Scheme 5.[38]

In a different direction, preliminary results suggest that **2** can serve as a precursor to polypyrrole films on electrodes.[39] Also, with alkylpyrrolyl complexes, electrophilic additions may generate quaternary carbon stereocenters in a diastereoselective fashion. Promising initial results have been obtained with 3-alkylindolyl complexes of $\{Re\}^+$.[13] Finally, species such as **10** might be elaborated to novel chiral semicorrins and related compounds.[40]

Summary

This study has shown that the *N*-pyrrolyl ligand in rhenium complex **2** is activated towards electrophilic attack. Furthermore, protonation triggers a remarkable metal–carbon bond forming rearrangement. Although mechanistic ambiguities remain, a new type of bond activation process involving formal [1,*n*] proton and metal shifts appears to be operative. These and other data given above clearly establish that *N*-pyrrolyl complexes will have a particularly fertile and useful reaction chemistry.

Experimental Section

General procedures were given in an earlier paper [19a]. Solvents not specified previously [19a] were used without purification. Reagents were used as received from common commercial sources. Cyclic voltammograms were recorded as described elsewhere [41].

Potassium Pyrrolide [12]: A Schlenk flask was charged with toluene (100 mL), freshly cut potassium (2.75 g, 70.3 mmol), pyrrole (12.5 mL, 180 mmol), and a stir bar. The mixture was refluxed with stirring. The molten potassium gave way to a white solid. After an additional 10 min, the mixture was cooled to room temperature. The solid was isolated by filtration, washed with toluene (3 × 20 mL), and dried under oil-pump vacuum to give potassium pyrrolide as a free-flowing white powder (7.01 g, 66.7 mmol, 95%).

[{Re}(NCH=CHCH=CH)] (2): A Schlenk flask was charged with [{Re}(OTf)] (**1**) (0.750 g, 1.08 mmol) [10a,11], THF (100 mL), and a stir bar. Then potassium pyrrolide (0.171 g, 1.62 mmol) was added with stirring. After 1 h, the mixture was filtered through a Celite plug. Solvent was removed from the filtrate by rotary evaporation (90–100 °C), and benzene (50 mL) was added. The mixture was filtered through a silica gel plug. Solvent was removed from the crimson filtrate by rotary evaporation (90–100 °C). The residue was crystallized from layered THF/ether to give **2** as bright red prisms, which were collected by filtration and dried under oil-pump vacuum (0.583 g, 0.956 mmol, 88%), M.p. 202 °C; UV/Vis (CH_2Cl_2): λ_{max} (ε) = 260 (8900 sh), 310 (2500 sh), 380 nm (930 sh); $C_{27}H_{24}N_2OPRe$ (609.7): calcd C 53.19, H 3.97; found C 53.13, H 3.99.

[{Re}(NCH=C(COCF$_3$)CH=CH)] (3): **A.** A Schlenk flask was charged with **2** (0.0730 g, 0.120 mmol), ether (50 mL), and a stir bar, and cooled to −80 °C (C_2H_5OH/CO_2). Then $(CF_3CO)_2O$ (0.0175 mL, 0.124 mmol) was added with stirring, and the cold bath was removed. After 1 h, $N(C_2H_5)_3$ (0.0175 mL, 0.126 mmol) was added. After 1 h, the mixture was filtered through a silica gel plug. Solvent was removed from the filtrate by rotary evaporation. The residue was crystallized from layered THF/pentane to give **3** as light yellow needles, which were collected by filtration and dried under oil-pump vacuum (0.0651 g, 0.0922 mmol, 77%), M.p. 233–235 °C (decomp.): $C_{29}H_{23}F_3N_2O_2PRe$ (705.7): calcd C 49.36, H 3.28; found C 49.49, H 3.33.

B. A 5 mm NMR tube was charged with **2** (0.0221 g, 0.0362 mmol) and CD_2Cl_2 (0.7 mL), capped with a septum, and cooled to −80 °C. Then $(CF_3CO)_2O$ (0.0052 mL, 0.037 mmol) was added. The tube was quickly transferred to a −80 °C probe. Data: see text. After the probe had been warmed to ambient temperature for the last time, $N(C_2H_5)_3$ (0.0050 mL, 0.036 mmol) was added.

[{Re}(NC(C(CO$_2$CH$_3$)=CH(CO$_2$CH$_3$))=CHCH=CH)] (5): **A.** A Schlenk flask was charged with **2** (0.514 g, 0.843 mmol), CH_2Cl_2 (100 mL), and a stir bar. Then

DMAD (0.200 mL, 1.63 mmol) [10b] was added with stirring. After 1 h, the mixture was filtered through a silica gel plug. The filtrate was concentrated to 5 mL and added to pentane (400 mL). The precipitate was collected by filtration, washed with pentane (3 × 5 mL), and dried under oil-pump vacuum to give **5** as a golden red powder (0.437 g, 0.583 mmol, 69%; 93:7 mixture of C=C isomers) [14]. M.p. 174–176 °C (decomp.); $C_{33}H_{30}N_2O_5PRe$ (751.8): calcd C 52.72, H 4.02; found C 52.83, H 4.11.

B. A 5 mm NMR tube was charged with **2** (0.0219 g, 0.0289 mmol) and CD_2Cl_2 (0.7 mL), capped with a septum, and cooled to −80 °C. Then DMAD (0.010 mL, 0.081 mmol) was added. The tube was quickly transferred to a −80 °C probe. Data: see text.

[{Re}(N=CHCH=CHCH$_2$)]$^+$X$^-$ (7$^+$X$^-$): **A**. A Schlenk flask was charged with **2** (0.063 g, 0.103 mmol), ether (50 mL), and a stir bar. Then TfOH (0.011 mL, 0.12 mmol) was slowly added with stirring. After 10 min, the precipitate was collected by filtration, washed with ether (3 × 10 mL), and dried under oil-pump vacuum to give **7**$^+$TfO$^-$ as a yellow powder (0.070 g, 0.092 mmol, 89%), M.p. 132–134 °C (decomp.); $C_{28}H_{25}F_3N_2O_4PReS$ (759.8): calcd C 44.27, H 3.32; found C 44.18, H 3.28.

B. Complex **2** (0.061 g, 0.10 mmol), ether (50 mL), and $HBF_4 \cdot OEt_2$ (0.020 mL, 0.19 mmol) were combined in a procedure analogous to that given for **7**$^+$TfO$^-$. An identical workup gave **7**$^+$BF$_4^-$ as a canary-yellow powder (0.058 g, 0.083 mmol, 83%), M.p. 180–181 °C (decomp.). Anal. calcd for $C_{27}H_{25}BF_4N_2OPRe$ (697.5): calcd C 46.49, H 3.61; found C 46.31, H 3.65.

[{Re}(C=NHCH$_2$CH=CH)]$^+$TfO$^-$ (9$^+$X$^-$): **A**. A Schlenk flask was charged with **7**$^+$TfO$^-$ (0.050 g, 0.066 mmol), CH_2Cl_2 (2 mL), and a stir bar. The solution was stirred for 4 d. Then heptane (50 mL) was slowly added. The precipitate was collected by filtration, washed with heptane (2 × 5 mL) and dried under oil-pump vacuum to give **9**$^+$TfO$^-$ as a red powder (0.045 g, 0.059 mmol, 90%), M.p. 115 °C (decomp.); UV/Vis (CH_2Cl_2): λ_{max} (ε) = 268 (6300 sh), 346 (7200 pk), 518 nm (460 pk); MS (7 kV, (+)-FAB, Ar, 3-nitrobenzyl alcohol/CH_2Cl_2 matrix): *m/z* (%): 611 (100) [M^+], 544 (20) [$M^+ - NC_4H_5$]. A portion was dissolved in CH_2Cl_2 (4 mL) and layered with ether/hexane (4/2 mL). After 2 d, dark red prisms of **9**$^+$TfO$^-$ were collected by filtration and dried under oil-pump vacuum. Anal. calcd for $C_{28}H_{25}F_3N_2O_4PReS$ (759.8): calcd C 44.27, H 3.32; found C 44.29, H 3.28.

B. A Schlenk flask was charged with **1** (0.225 g, 0.325 mmol), toluene (50 mL), pyrrole (0.200 mL, 2.88 mmol), and a stir bar, and was fitted with a condenser. The solution was refluxed for 24 h. Solvent was removed under oil-pump vacuum. The residue was washed with heptane (4 × 10 mL) and dried under oil-pump vacuum to give **9**$^+$TfO$^-$ (0.228 g, 0.300 mmol, 92%).

C. A 5 mm NMR tube was charged with **10** (0.090 g, 0.15 mmol) and CD_2Cl_2 (0.6 mL), capped with a septum, and cooled to −80 °C. Then TfOH (0.013 mL, 0.15 mmol) was slowly added. The tube was quickly transferred to a −80 °C probe. Data: see text.

D. Complex **7**$^+$BF$_4^-$ (0.050 g, 0.072 mmol) was treated as described for **7**$^+$TfO$^-$ in procedure **A**. An identical workup gave **9**$^+$BF$_4^-$ as a crimson powder (0.048 g, 0.069 mmol, 96%). M.p. 129–132 °C (decomp.); UV/Vis (CH_2Cl_2): λ_{max} (ε) = 268 (6600 sh), 346 (7400 pk), 518 nm (1200 pk).

[{Re}(C=CHCH=CHNH)] (10): A Schlenk flask was charged with **9**$^+$TfO$^-$ (0.201 g, 0.265 mmol), THF (25 mL), KH (0.201 g, 5.02 mmol), and a stir bar. The red mixture was stirred. After 5 min, the brown sample was filtered through a Celite plug. Solvent was removed from the filtrate under oil-pump vacuum, and ether (300 mL) was added. The mixture was filtered through a Celite plug. Solvent was removed from the filtrate under oil-pump vacuum. The residue was washed with ether (4 × 2 mL) and dried under oil-pump vacuum to give **10** as a red powder (0.110 g, 0.180 mmol, 68%). M.p. 124–129 °C (decomp.); MS (EI): *m/z* (%): 610 (2) [M^+], 579 (9) [$M^+ - NO - 1$], 262 (100) [Ph_3P^+]; anal. calcd for $C_{27}H_{24}N_2OPRe$ (609.7): calcd C 53.19, H 3.97; found C 52.95, H 4.03.

Other NMR-Monitored Reactions: **A**. Separate 5 mm NMR tubes were charged with **7**$^+$TfO$^-$ (0.038 g, 0.050 mmol) or **7**$^+$BF$_4^-$ (0.035 g, 0.050 mmol) and CD_2Cl_2 (0.6 mL), and capped with septa. Another tube was similarly charged with **1** (0.035 g, 0.050 mmol), CD_2Cl_2 (0.6 mL), and pyrrole (0.0045 mL, 0.065 mmol). ^1H and ^{31}P NMR spectra were periodically recorded. Data: see Table 4.

B. A 5 mm NMR tube was charged with **1** (0.035 g, 0.050 mmol), toluene (0.6 mL), and pyrrole (0.020 mL, 0.30 mmol), capped with a septum, and kept at 100 °C. Aliquots were periodically removed, taken to dryness, and dissolved in CD_2Cl_2. Then ^1H and ^{31}P NMR spectra were recorded. Data: see text.

C. A 5 mm NMR tube was charged with pyrrole (0.0020 mL, 0.029 mmol) and CD_2Cl_2 (0.7 mL), capped with a septum, and cooled to −100 °C. Then $(CF_3CO)_2O$ (0.0042 mL, 0.030 mmol) was added. The tube was quickly transferred to a −100 °C probe. Data: see text.

Crystallography: Data were collected on dark red prisms of **2** (from layered CH_2Cl_2/pentane) and **9**$^+$TfO$^-$ as outlined in Table 2 (Syntex P$\bar{1}$ diffractometer). Cell constants were obtained from 25 reflections with $15 < 2\theta < 20°$ (**2**) and 30 reflections with $10 < 2\theta < 20°$ (**9**$^+$TfO$^-$). Space groups were determined from systematic absences (**2**, *h0l* $h + l = 2n + 1$, *0k0* $k = 2n + 1$; **9**$^+$TfO$^-$, *h0l* $h + l = 2n + 1$, *0k0* $k = 2n + 1$) and subsequent least squares refinement. Lorentz, polarization, and empirical absorption (ψ scans) corrections were applied. The structures were solved by standard heavy-atom techniques with the SDP-VAX package [42]. Nonhydrogen atoms were refined with anisotropic thermal parameters. All hydrogen atoms were located and added to the structure factor calculations. Those of **2** (but not **9**$^+$TfO$^-$) were refined. Scattering factors, and $\Delta f'$ and $\Delta f''$ values, were taken from ref. [43,44].

MO calculations: Extended Hückel MO calculations were conducted on a Tektronix CAChe workstation (version 3.6) using parameters given previously [25]. Geometries were taken from the crystal structures, and PH_3 ligands were given 1.3 Å phosphorus–hydrogen bond lengths and tetrahedral bond angles. Energies in Figure 4 were calculated every 2° (top panel) and 2–10° (bottom) [27a,b].

Acknowledgement: We thank the DOE for support of this research.

Received: January 26, 1995 [F69]

[1] a) P. L. Pauson, A. R. Qazi, *J. Organomet. Chem.* **1967**, *7*, 321; b) A. Efraty, N. Jubran, A. Goldman, *Inorg. Chem.* **1982**, *21*, 868; c) R. V. Bynum, H.-M. Zhang, W. E. Hunter, J. L. Atwood, *Can. J. Chem.* **1986**, *64*, 1304 and references therein; d) A. Salifoglou, A. Simopoulos, A. Kostikas, R. W. Dunham, M. G. Kanatzidis, D. Coucouvanis, *Inorg. Chem.* **1988**, *27*, 3394; e) E. Carmona, P. Palma, M. Paneque, M. L. Poveda, *Organometallics* **1990**, *9*, 583 and references therein; f) J. J. H. Edema, S. Gambarotta, A. Meetsma, F. van Bolhuis, A. L. Spek, W. J. J. Smeets, *Inorg. Chem.* **1990**, *29*, 2147; g) J. Zakrzewski, C. Giannotti, *J. Organomet. Chem.* **1990**, *388*, 175; h) F. T. Lapido, J. S. Merola, *Inorg. Chem.* **1990**, *29*, 4172; i) R. D. Simpson, R. G. Bergman, *Organometallics* **1992**, *11*, 3980; j) W. D. Jones, L. Dong, A. W. Meyers, *Organometallics* **1995**, *14*, 855.

[2] *Pyrroles*, Part 1 (Ed.: R. A. Jones), Wiley, New York, **1990**: a) pp. 295–303, b) pp. 549–728, c) pp. 305–308.

[3] a) B. L. Bray, P. H. Mathies, R. Naef, D. R. Solas, T. T. Tidwell, D. R. Artis, J. M. Muchowski, *J. Org. Chem.* **1990**, *55*, 6317; b) H. Seino, Y. Ishii, M. Hidai, *J. Am. Chem. Soc.* **1994**, *116*, 7433.

[4] For example, vitamin B_{12} contains four partially saturated pyrrole rings, each with two or three stereocenters. See F.-P. Montforts, B. Gerlach, F. Höper, *Chem. Rev.* **1994**, *94*, 327.

[5] B. R. Sanders, R. J. Fleming, K. S. Murray, *Chem. Mater.* **1995**, *7*, 1082.

[6] J. L. Sessler, G. Hemmi, T. D. Mody, T. Murai, A. Burrell, S. W. Young, *Acc. Chem. Res.* **1994**, *27*, 43.

[7] a) R. M. Laine, *Catal. Rev. Sci. Eng.* **1983**, *25*, 459; b) H. Schulz, M. Schon, N. M. Rahman in Studies in Surface Science and Catalysis, Vol. 27 (Ed.: L. Cerveny), Elsevier, New York, **1986**, Chap. 6.

[8] G. B. Richter-Addo, A. D. Knight, M. A. Dewey, A. M. Arif, J. A. Gladysz, *J. Am. Chem. Soc.* **1993**, *115*, 11863.

[9] T. J. Johnson, A. M. Arif, J. A. Gladysz, *Organometallics* **1993**, *12*, 4728.

[10] Abbreviations: a) {Re} = (η^5-C_5H_5)Re(NO)(PPh$_3$); b) OTf = OSO_2CF_3; c) DMAD = $CH_3O_2CC{\equiv}CCO_2CH_3$.

[11] J. H. Merrifield, J. M. Fernández, W. E. Buhro, J. A. Gladysz, *Inorg. Chem.* **1984**, *23*, 4022.

[12] C. F. Hobbs, C. K. McMillin, E. P. Papadopoulos, C. A. Vander Werf, *J. Am. Chem. Soc.* **1962**, *84*, 43.

[13] T. J. Johnson, A. M. Arif, J. A. Gladysz, *Organometallics* **1994**, *13*, 3182.

[14] a) Complex **4**$^+$$CF_3CO_2^-$ might rapidly rearrange to other carbon or carbonyl protonated derivatives of **3**. These data establish the rapid time scale of reaction, but not the identities of the observed intermediates; b) This assignment was based upon the similar N(CH)CH=CH ^1H NMR chemical shifts and coupling constants (Table 1). From shielding parameters for vinylic protons, the major isomer likely has a *Z* C=C linkage: R. M. Silverstein, G. C. Bassler, T. C. Morrill, *Spectrometric Identification of Organic Compounds*, 5th ed., Wiley, New York, **1991**, Table D. 1. Partial data for *E* isomer: ^1H NMR: δ = 6.66 (s, =C*H*CO$_2$CH$_3$), 6.23 (m, NCH), 5.97 (dd, J = 3.3, 1.8 Hz, NC(C)CH), 5.60 (dd, J = 3.3, 2.4 Hz, NCHC*H*), 5.17 (s, C_5H_5), 3.83, 3.67 (2s, CH_3); $^{31}P\{^1H\}$ NMR: δ = 17.4 (s).

[15] a) R. Dunkel, C. L. Mayne, R. J. Pugmire, D. M. Grant, *Anal. Chem.* **1992**, *64*, 3133; b) R. Dunkel, C. L. Mayne, M. P. Foster, C. M. Ireland, D. Li, N. L. Owen, R. J. Pugmire, D. M. Grant, *Anal. Chem.* **1992**, *64*, 3150.

[16] a) Spectra were recorded on a Varian VXR 500 spectrometer (**5**, CD_2Cl_2, −50 °C; **7**$^+$TfO$^-$, CD_2Cl_2, −85 °C); b) These experiments also give $^1J(^{13}C-^{13}C)$ values (Hz): **5**: =*C*HCO 77.0(2); =*C*HCO 77.0(2), 73.6(2); *C*=CHCO 73.6(2), 70.2(2), 67.7(3); OC*C*=CH 70.2(2); OCC*C*N 67.7(3), 63.2(2); NCH=C*H*C 63.2(2), 53.7(3); NCH=*C*H 53.7(3), 59.5(3); NC*H*=CH 59.5(3). **7**$^+$TfO$^-$: CH=N 49.1(7); *C*=CH=N 49.1(7), 61.4(7); =*C*HCH$_2$ 61.4(7), 37.7(9); CH_2 37.7(9).

[17] R. M. Acheson, J. M. Vernon, *J. Chem. Soc.* **1963**, 1008.

[18] D. M. Doddrell, D. T. Pegg, M. R. Bendall, *J. Magn. Reson.* **1982**, *48*, 323.

[19] a) D. A. Knight, M. A. Dewey, G. A. Stark, B. K. Bennett, A. M. Arif, J. A. Gladysz, *Organometallics* **1993**, *12*, 4523; b) W. R. Cantrell Jr., G. B. Richter-Addo, J. A. Gladysz, *J. Organomet. Chem.* **1994**, *472*, 195.

[20] a) Y. Chiang, E. B. Whipple, *J. Am. Chem. Soc.* **1963**, *85*, 2763; b) E. B. Whipple, Y. Chiang, R. L. Hinman, *J. Am. Chem. Soc.* **1963**, *85*, 26; c) $^{13}C\{^1H\}$ NMR (H_2SO_4): $\delta = 173.3$ (s, C=N), 160.1 (s), 128.2 (s), 62.7 (s, CH_2).

[21] M. A. Dewey, D. A. Knight, D. P. Klein, A. M. Arif, J. A. Gladysz, *Inorg. Chem.* **1991**, *30*, 4995.

[22] An alternative tautomer, $[\{Re\}(C{=}CHCH_2CH{=}NH)]^+X^-$, would have a ReC=CH linkage as opposed to the ReC=NH linkages in $\mathbf{8}^+X^-$ and $\mathbf{9}^+X^-$. Thus, the high degree of NMR chemical-shift homology evident in Table 1 would not be expected.

[23] a) M. M. P. Ng, W. R. Roper, L. J. Wright, *Organometallics* **1994**, *13*, 2563; b) G. R. Clark, M. M. P. Ng, W. Roper, L. J. Wright, *J. Organomet. Chem.* **1995**, *491*, 219; c) For chelate complexes that incorporate a *C*-pyrrolyl moiety, see N. P. Robinson, L. Main, B. K. Nicholson, *J. Organomet. Chem.* **1988**, *349*, 209.

[24] a) E. Söderbäck, *Acta Chem. Scand.* **1959**, *13*, 1221; b) G. N. O'Connor, J. V. Crawford, C.-H. Wang, *J. Org. Chem.* **1965**, *30*, 4090.

[25] a) G. S. Bodner, A. T. Patton, D. E. Smith, S. Georgiou, W. Tam, W.-K. Wong, C. E. Strouse, J. A. Gladysz, *Organometallics* **1987**, *6*, 1954; b) W. E. Buhro, B. D. Zwick, S. Georgiou, J. P. Hutchinson, J. A. Gladysz, *J. Am. Chem. Soc.* **1988**, *110*, 2427.

[26] J. I. Seeman, S. G. Davies, *J. Am. Chem. Soc.* **1985**, *107*, 6522.

[27] a) The rhenium–phosphorus conformations were not concurrently minimized. However, for selected points near the minima and maxima in Figure 4, energies were calculated as the rhenium–phosphorus bonds were rotated in 5° increments. Differences were less than 0.9 kcal mol^{-1}, and the positions of the minima were unaffected. b) Calculations on compounds with PPh_3 ligands gave minima essentially identical with those in Figure 4. c) In chiral molecules, the sign of a torsion angle arbitrarily depends upon the enantiomer selected. Hence, all of the torsion angles in this paper are expressed analogously to θ in Figure 4.

[28] a) R. Cordone, W. D. Harman, H. Taube, *J. Am. Chem. Soc.* **1989**, *111*, 5969; b) W. H. Myers, J. I. Koontz, W. D. Harman, *J. Am. Chem. Soc.* **1992**, *114*, 5684; c) L. M. Hodges, J. Gonzalez, J. I. Koontz, W. H. Myers, W. D. Harman, *J. Org. Chem.* **1993**, *58*, 4788; d) L. M. Hodges, M. W. Moody, W. D. Harman, *J. Am. Chem. Soc.* **1994**, *116*, 7931.

[29] We have been unable to devise a labeling experiment that would unambiguously distinguish the pathways in Scheme 6. For example, mechanism (b) might be probed with $\mathbf{7}^+X^-$ that is $^{13}C{=}N$ labeled. However, there is no obvious way to prepare such a compound. Even if it were accessible, it is likely that scrambling of the label into the CH_2 group would be faster than rearrangement.

[30] For theoretical studies of [1,5] sigmatropic shifts in tautomers of free pyrrole, see S. M. Bachrach, *J. Org. Chem.* **1993**, *58*, 5414.

[31] a) Several rhenium η^1-cyclopentadienyl complexes have been isolated. These show one C_5H_5 ^1H and ^{13}C NMR signal at room temperature. This *requires* a rapid (net) [1,5] sigmatropic shift of rhenium. b) C. P. Casey, W. D. Jones, *J. Am. Chem. Soc.* **1980**, *102*, 6154; c) C. P. Casey, J. M. O'Connor, K. J. Haller, *J. Am. Chem. Soc.* **1985**, *107*, 1241.

[32] a) M. J. Robertson, C. J. White, R. J. Angelici, *J. Am. Chem. Soc.* **1994**, *116*, 5190; b) C. J. White, R. J. Angelici, *Organometallics* **1994**, *13*, 5132.

[33] a) P. C. Cagle, A. M. Arif, J. A. Gladysz, *J. Am. Chem. Soc.* **1994**, *116*, 3655; b) O. Meyer, A. M. Arif, J. A. Gladysz, *Organometallics* **1995**, *14*, 1844.

[34] Variants involving proton abstraction from η^2 2*H*- or 3*H*-pyrrole ligands can also be considered. Indeed, cationic alkene complexes of $\{Re\}^+$ are deprotonated to neutral vinyl complexes upon treatment with tBuO$^-$K$^+$: T. S. Peng, J. A. Gladysz, *Organometallics* **1995**, *14*, 898, and references therein.

[35] J. March, *Advanced Organic Chemistry*, 4th ed., Wiley, New York, **1992**, Table 1.5.

[36] a) W. E. Crowe, S. L. Schreiber, in *Advances in Metal-Organic Chemistry*, Vol. 2 (Ed.: L. S. Liebeskind), JAI, Greenwich, Conn., **1991**, p. 247, and references therein; b) S. G. Davies, A. J. Smallridge, *J. Organomet. Chem.* **1990**, *397*, C13, and references therein.

[37] Available solution-phase NMR data appear to support this conclusion. For IR data, see S. C. Mackie, M. C. Baird, *Organometallics* **1992**, *11*, 3712.

[38] F. Kvietok, V. Allured, V. Carperos, M. Rakowski DuBois, *Organometallics* **1994**, *13*, 60.

[39] M. Brady, unpublished data, University of Utah.

[40] A. Pfaltz, *Acc. Chem. Res.* **1993**, *26*, 339.

[41] M. Brady, W. Weng, J. A. Gladysz, *J. Chem. Soc. Chem. Commun.* **1994** 2655.

[42] B. A. Frenz, *The Enraf-Nonius CAD4SDP—A Real-Time System for Concurrent X-ray Data Collection and Crystal Structure Determination. In Computing and Crystallography* (Eds.: H. Schenk, R. Olthof-Hazelkamp, H. van Konigsveld, G. C. Bassi), Delft University, Delft, Holland, **1978**, pp. 64–71.

[43] D. T. Cromer, J. T. Waber in *International Tables for X-ray Crystallography*, Vol. IV (Eds.: J. A. Ibers, W. C. Hamilton), Kynoch, Birmingham, England, **1974**, pp. 72–98 and 149–150, Tables 2.2 B and 2.3.1.

[44] Further details of the crystal structure investigation may be obtained from the Director of the Cambridge Crystallographic Data Centre, 12 Union Road, GB-Cambridge CB2 1EZ (UK), on quoting the full journal citation.

[45] W. E. Buhro, S. Georgiou, J. M. Fernández, A. T. Patton, C. E. Strouse, J. A. Gladysz, *Organometallics* **1986**, *5*, 956.